PAPER • OPEN ACCESS

Hybrid fusion using Gram Schmidt and Curvelet transforms for satellite images

To cite this article: M Hammad *et al* 2021 *IOP Conf. Ser.: Mater. Sci. Eng.* **1172** 012016

Hybrid fusion using Gram Schmidt and Curvelet transforms for satellite images

M Hammad[1], T Ghoniemy[1], T Mahmoud[1] and A Amein[2]

[1]Electrical Engineering, Military Technical College, Cairo, Egypt.
[2]Electrical Engineering, Senior IEEE, FISCS, October 6 University, Cairo, Egypt.

E-mail: Radok2003@hotmail.com

Abstract. Optical satellites generally provide high-resolution panchromatic but low-resolution multispectral images which provide structural details of features and spectral information respectively. Nowadays, fusion of the two types of resolutions, to have complementary information, becomes increasingly essential for many applications such as microscopic, astronomical and satellite imagery. In this paper, a novel hybrid pixel-level image fusion method is proposed for benefiting from both panchromatic (PAN) and multispectral (MUL) images. The proposed method integrates Gram Schmidt (GS) and curvelet transforms (CVT), by the aid of local energy and maximum fusion rules, for reducing individual method limitations and achieving both better spectral consistency and spatial details preservation. After a pre-processing stage, orthonormal bases are obtained for low spatial resolution images by using GS transform. Then, high-resolution and low-resolution images are fused using CVT by the aid of histogram matching. Finally, the fused image is obtained by applying both curvelet and GS inverse transforms. The performance of the proposed method is evaluated using publicly available Pleiades benchmark-datasets. Consequently, the spectral and spatial qualities of the fused images are assessed subjectively as well as objectively using different quality metrics. Moreover, the proposed method is compared with state-of-the-art fusion techniques and results show the robustness of the proposed method that has the best result in spatial and spectral evaluation metrics such as, Quality with No Reference (QNR), Peak Signal to Noise Ratio (PSNR), Standard Deviation (SD), Entropy (ENT) and Spectral Correlation Coefficient (SCC) metrics.

1. Introduction

Remote sensing satellite images have different types of resolutions due to the technical and physical constrains of satellites. Optical satellites have high spatial/low spectral resolution images over wide bandwidth and low spatial/high spectral resolution images over narrow bandwidth [1]. Therefore, there is a need to integrate the desired information from various images into a single more informative image. This is performed in order to have a clear understanding of these images for better using in different applications such as urban mapping, topographic map updating, mineral exploitation, land use/land cover mapping and natural hazards and disasters [1], and providing efficient decision-making. Accordingly, image fusion meets these needs. It achieves credibility by preservation of all relevant information, elimination of irrelevant information and noise. Moreover, fusion process should succeed in minimizing artifacts, shift and rotational invariance, stability, consistency and reducing time complexity [2]. Fused image is expressed mathematically as follows:

$$\mathrm{FI} = \mathrm{F}(\mathrm{I}_1, \mathrm{I}_2, \dots, \mathrm{I}_\mathrm{N}) = \mathrm{c}_1\mathrm{I}_1 + \mathrm{c}_2\mathrm{I}_2 + \cdots + \mathrm{c}_\mathrm{N}\mathrm{I}_\mathrm{N} \quad (1)$$

Where FI is the fused image, $I_1, I_2, \ldots, I_N$ are N input images, F represents the fusion rule, and c's are constants such that $\sum_{n=1}^{N} c_n = 1$.

Nowadays, a huge number of image fusion techniques have been proliferated that are classified in several distinct ways such as acquisition mode, level of fusion, fusion domain that can be either spatial or transform, type of resolutions which the fusion process emphasizes, and type of images which are utilized in the fusion process [3-6]. On the basis of a level at which fusion is carried out, fusion methods are classified into three categories namely pixel level, feature level, and decision level [3] as shown in figure 1.

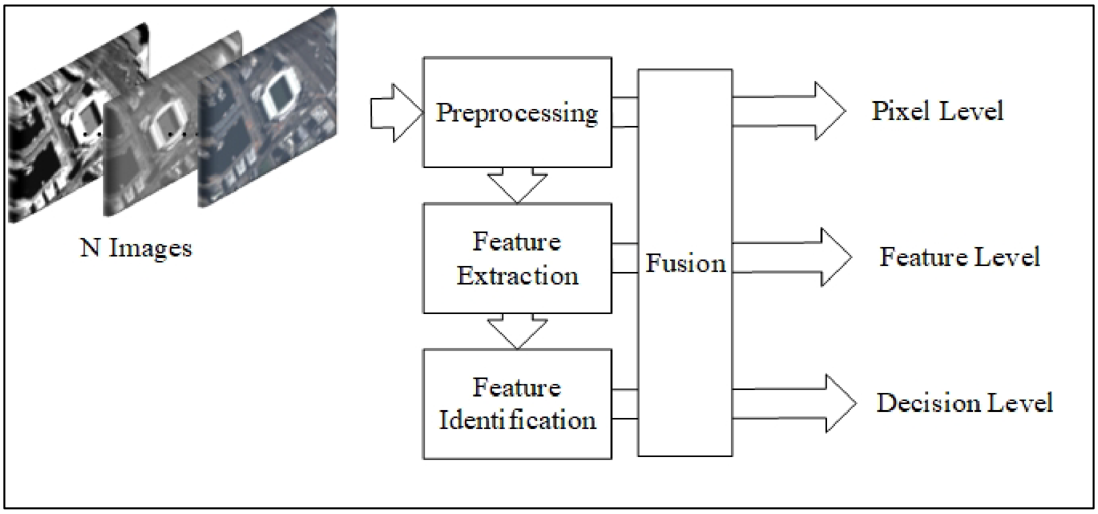

Figure 1. Fusion levels.

The reset of this paper is structured as follows. Section 2 discusses the related work. Section 3 overviews the methodology. Section 4 illustrates the data description and experimental setup. Section 5 gives the experimental results and discussion. Section 6 the conclusion is given. In Section 7, the future work is proposed.

2. Related works

Pixel level classification is relevant to this paper that is categorized into [3, 7]: (1) component substitution based (CS), (2) multiscale decomposition (MSD), (3) hybrid methods, and (4) model-based methods. CS-based methods project the low spatial resolution image into other space in which the spatial and spectral components are separated, and then the spatial component is substituted by high spatial component from high spatial resolution image. CS-based methods have high spatial fidelity, but high spectral distortion. Intensity-Hue-Saturation (IHS), principal component analyses (PCA), Brovey transform (BT), and Gram-Schmidt (GS) belong to this category. MSD-based methods try to overcome the spectral deformation problem of CS-based category and achieves better signal to noise ratio at the cost of complexity. It differs from CS-based category by the spatial details extraction method. To achieve the main target of image fusion, CS-based methods and MSD-based methods are combined to synergy the advantages of these categories and relieving individual method limitations, namely, hybrid category [7]. Typical examples of hybrid category are IHS–BT fusion, wavelet-IHS fusion, wavelet-PCA fusion, modified BT-wavelet fusion, curvelet-PCA fusion and Laplacian Filtering and Multiple Regression, etc. In [8], SAR and multispectral images are fused using Spare Representation (SR) and non-subsampled Shearlet transform (NSST) that preserve the edge and detailed information, as well as sharpness and contrast. In [9], Xiaole Ma presents new fusion method based on SR and guided filtering, the proposed approach is evaluated over a different kind of images, it preserve detail information and has a good visual analysis however, this method is inefficient if the low frequency in the image is greater than its high frequency. In [10], SAR and optical images fusion using IHS and wavelet transform Integration is introduced that made the image more sharpener and interpretable. In [11] Multispectral and panchromatic image are fused using IHS and CVT with different fusion rules that ensure the efficiency of the integration method. In [12], a combination of PCA and CVT is proposed that preserves spectral and improves spatial information. CVT is also combined with adaptive neuro-fuzzy inference system in [13] for improving the fusion process.

Motivated by the advantages of hybrid category, a new integration of GS-based and CVT-based methods is proposed as a fusion method in this paper, which uses matching criteria with a predefined threshold and local energy as a saliency measure. The proposed fusion algorithm is analyzed and compared visually and statistically with numerous CS-based and MSD-based methods over ten panchromatic (PAN) and multispectral (MUL) Pleiades satellites samples images. Result reveals that the proposed method significantly enhances the spectral as well as the spatial information.

3. Methodology

The proposed fusion method combined GS-based and CVT-based methods to overcome the limitation of individual method and have high spatial details while preserving the spectral information as much as possible as will be illustrated in the following sections. Table 1 gives the definition of the used symbols.

Table 1. Definition of the used symbols.

symbol	definition	symbol	definition
b	Number of low spatial resolution image band	$EHR_{x,y}$	Local energy around center coefficient of high resolution image
GS	Gram Schmidt component $1 \leq GS \leq$ b+1	$ELR_{x,y}$	Local energy around center coefficient of low resolution image
HR_{sim}	Simulated high spatial resolution image	T	threshold
LR	Low spatial resolution image	W_{max}	Max weight
$C_{x,y}$	Curvelet coefficient	W_{min}	Min weight
$CHR_{x,y}$	Curvelet coefficient of high spatial resolution image	SD	Average standard deviation of image
$CLR_{x,y}$	Curvelet coefficient of low spatial resolution image	$Mean$	Average mean of image
j	Scale decomposition	D_λ	Spatial distortion
$\emptyset[x,y]$	Curvelet function	D_S	Spectral distortion
θ	Orientation of curvelet	L	The dynamic range of the image being analyzed
x, y	Pixel location in image	R	Referenced image
$k1, k2$	Spatial location of curvelets	FI	Fused image
$I[x,y]$	Input image	μ_{FI}	Local mean of image FI
m	Number of rows in image	μ_R	Local mean of image R
n	Number of column in image	$p(g)$	The probability of occurrence of g^{th} gray level
$\widehat{LR}$	Resampled low spatial resolution image	RF	Row frequency
$[X,Y]$	Dimension of used local window	CF	Column frequency
M	Matching function		

3.1. GS-based method

Since the published patent in [14], GS-based fusion method becomes one of the most interesting fusion methods [1, 15, 16]. First a simulated low-spatial resolution from the high spatial resolution image is computed, then GS-transform is applied to the simulated result and the low spatial resolution image bands as in equations (2- 5) [1], the simulated result is employed as a first component and the remaining components are computed orthogonal to it for solving the radiometric accuracy shortage in PCA-based fusion method, so it is described as a generalized PCA-based method [3]. Then the high spatial resolution image band replaces the first Gram Schmidt band. Finally, an inverse Gram Schmidt transform is applied to create the fused image. Its advantages are high preserving spectral information with high spatial details and deals with not limited numbers of images.

$$GS_1 = HR_{sim} \tag{2}$$

$$GS_2 = \widehat{LR}_1 - \frac{\langle HR_{sim} | \widehat{LR}_1 \rangle}{\langle HR_{sim} | HR_{sim} \rangle} \times HR_{sim} \tag{3}$$

$$GS_3 = \widehat{LR}_2 - \frac{\langle HR_{sim} | \widehat{LR}_2 \rangle}{\langle HR_{sim} | HR_{sim} \rangle} \times HR_{sim} - \frac{\langle GS_2 | \widehat{LR}_2 \rangle}{\langle GS_2 | GS_2 \rangle} \times GS_2 \tag{4}$$

$$\vdots$$

$$GS_{b+1} = \widehat{LR}_b - \frac{\langle HR_{sim} | \widehat{LR}_b \rangle}{\langle HR_{sim} | HR_{sim} \rangle} \times HR_{sim} - \sum_{k=1}^{b} \frac{\langle GS_k | \widehat{LR}_k \rangle}{\langle GS_k | GS_k \rangle} \times GS_k \tag{5}$$

3.2. CVT-based method

Curvelet transform is a multi-scale representation of image at different angle, and is a higher dimensional generalization of the wavelet transform that overcomes its limitation. CVT had been preceded through many development stages beginning from the derivation from ridge-wave theory that is complex until the second generation namely fast discrete curvelet transform algorithm that can be implemented in two ways via unequally spaced fast Fourier transform or wrapping function. In this work, a fast discrete curvelet transform algorithm is used via wrapping method which is faster and widely used [11, 12, 17]. These curvelets are arranged in various orientation and scale from (course to fine), this arrangement ensures that the entire image plane is covered to avoid signal losses as shown in figure 2.

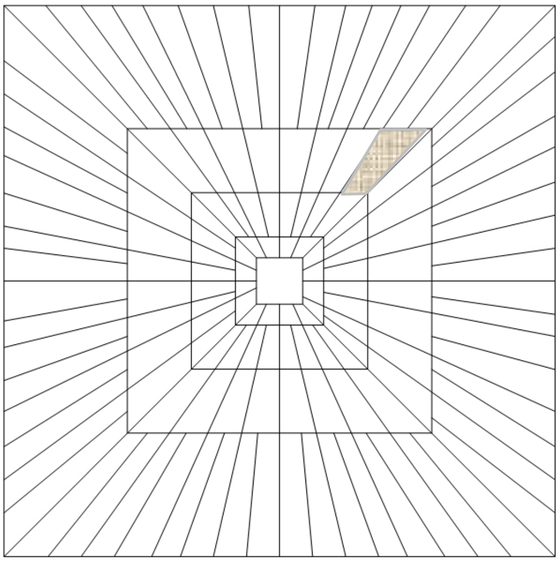

Figure 2. Basic digital tiling of curvelet transform frequency spectrum [18].

In general CVT can be expressed in time domain as in the following equation:

$$C(j,\theta,k1,k2) = \sum_{\substack{0\le x\le m\\ 0\le y\le n}} I\,[x,y]\,.\,\emptyset_{j,\theta,k1,k2}[x,y] \tag{6}$$

In figure 2, an example of 5 level curvelet digital tiling and the shaded wedged at scale 4 and at orientation 5, the center square gives approximation curvelet coefficient and the other scales give detailed curvelet coefficient.

3.3. The proposed GS-CVT method

The main contribution of this paper is to develop fusion algorithm capable of preserving the spectral as well as the spatial information. This work integrates the advantage of two fusion methods (CVT and GS) with suitable fusion rule as illustrated in the following steps, and in figure 3:

1- Resampling the low spatial resolution image with one of the interpolation methods to have the same size as high spatial resolution image. Bicubic interpolation method is used in this paper.

2- Simulated low-spatial resolution from the high spatial resolution image is computed using gaussian filter, the blurred output of the filter is used as the first component in the next step.

3- GS-transform is applied to the simulated result from step 2 and the orthogonal low spatial resolution image bands as in equations (2- 5).

4- Histogram matching is applied on the high spatial resolution image in order to have the same mean and variance of the low spatial resolution image bands GS-components.

5- Curvelet transform is applied on both the low spatial resolution image bands GS-components and high spatial resolution output from histogram matching in step 4, and the decomposition coefficients are obtained.

6- Decomposition coefficients output from curvelet transform for both images are divided to three layers, low frequency layer namely coarse-scale layer, detail scale layer, and fine scale layer.

7- The selection of fusion rule is a crucial factor for success of image fusion algorithm, this paper applies different fusion rules for each layer to rich the information of the final fused image as follows:

a- Low frequency layer fusion rule: the energy distribution of image is reflected by its low frequency, so local energy based method is used. First matching function M is computed over the low and high spatial resolution images bands for each coefficient $[x,y]$over local neighborhood $[X,Y]$ in j^{th} level of decomposition

$$M^j_{x,y} = \frac{2\sum_X\sum_Y CHR^j_{x+X,y+Y}CLR^j_{x+X,y+Y}}{EHR^j_{x,y}ELR^j_{x,y}} \tag{7}$$

The local energy at center coefficient is:

$$E^j_{x,y} = \sum_{x-X}^{x+X}\sum_{y-Y}^{y+Y} C^2_{x,y} \tag{8}$$

If the matching function value at a certain coefficient exceeds a predefined threshold T, then the coefficients of maximum local energy function are chosen, else if the matching function value is below that threshold, a weighted addition of coefficients is taken to generate fused coefficients. The shifted sigmoid function is used for the weights to ensure that the weights fall in range from [0, 1] according to the matching values. The following equation describes fusion rule for low frequency coefficients:

$$W_{max} = 2\times\left(\frac{1}{(1+e^{-M})-0.5}\right) \tag{9}$$

$$W_{min} = 1 - W_{max} \tag{10}$$

$$C_{x,y}^{j} = \begin{cases} CLR_{x,y}^{j}, & M_{x,y}^{j} > T \ , ELR_{x,y}^{j} > EHR_{x,y}^{j} \\ CHR_{x,y}^{j}, & M_{x,y}^{j} > T \ , ELR_{x,y}^{j} < EHR_{x,y}^{j} \\ W_{max} \times CLR_{x,y}^{j} + \ W_{min} \times CHR_{x,y}^{j}, & M_{x,y}^{j} < T \ , ELR_{x,y}^{j} > EHR_{x,y}^{j} \\ W_{max} \times CHR_{x,y}^{j} + \ W_{min} \times CLR_{x,y}^{j} & M_{x,y}^{j} < T \ , ELR_{x,y}^{j} < EHR_{x,y}^{j} \end{cases} \tag{11}$$

b- Detail scale layer, and fine scale layer coefficients fusion rule: decision map is used in order to obtain the detailed coefficients of images as it uses the average window based strategy to be more robust to mis-registration and choose the maximum strategy to get the fused coefficients map.

8- Apply inverse curvelet transform to reconstruct GS-components.

9- Apply inverse GS-transform in order to obtain the final fused image.

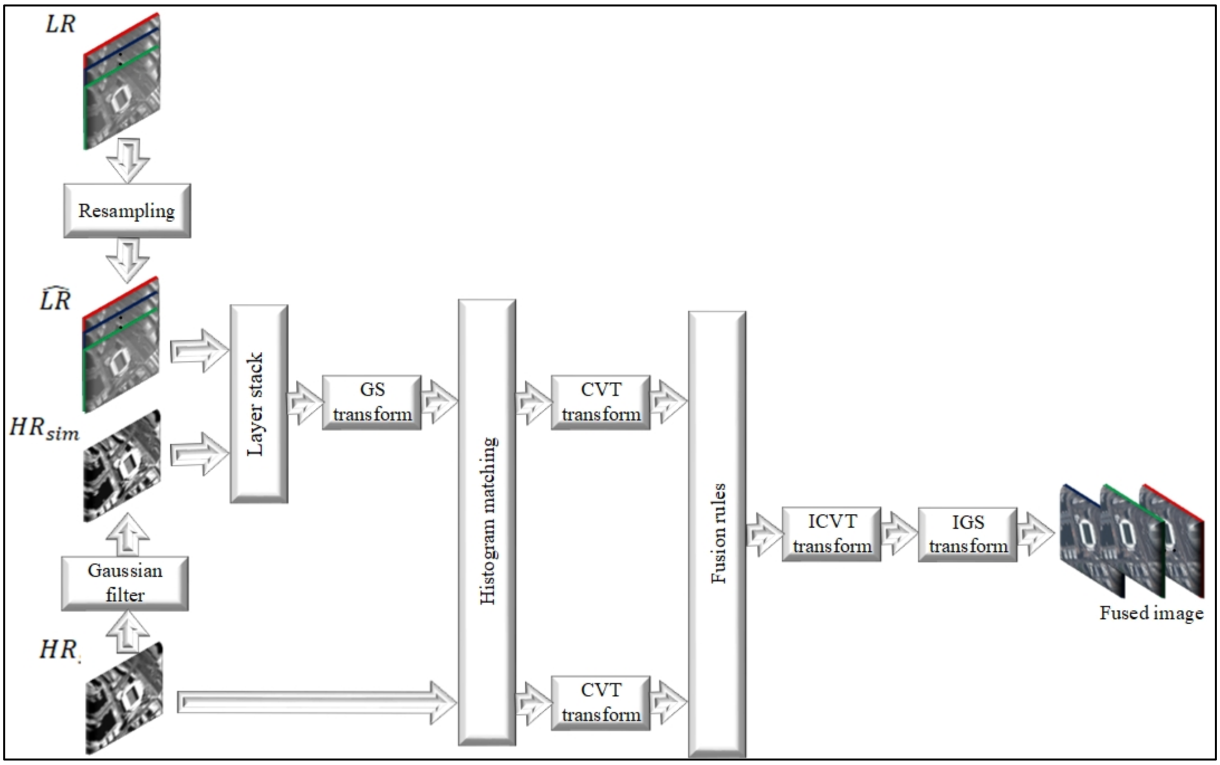

Figure 3. The proposed GS-CVT method flow chart.

4. Experimental setup

4.1. Dataset description and preprocessing

The proposed method is evaluated over ten pairs of Pleiades dataset as shown in figure 4, which is downloaded from [19] with the specifications shown in table 2. Dataset images size are 512×512 pixel for panchromatic images and 128×128 pixel for multispectral images as shown in figure 4. All the images are pre-processed such that they are registered then multispectral images are resampled using bicubic interpolation method by using ERDAS/ MATLAB software.

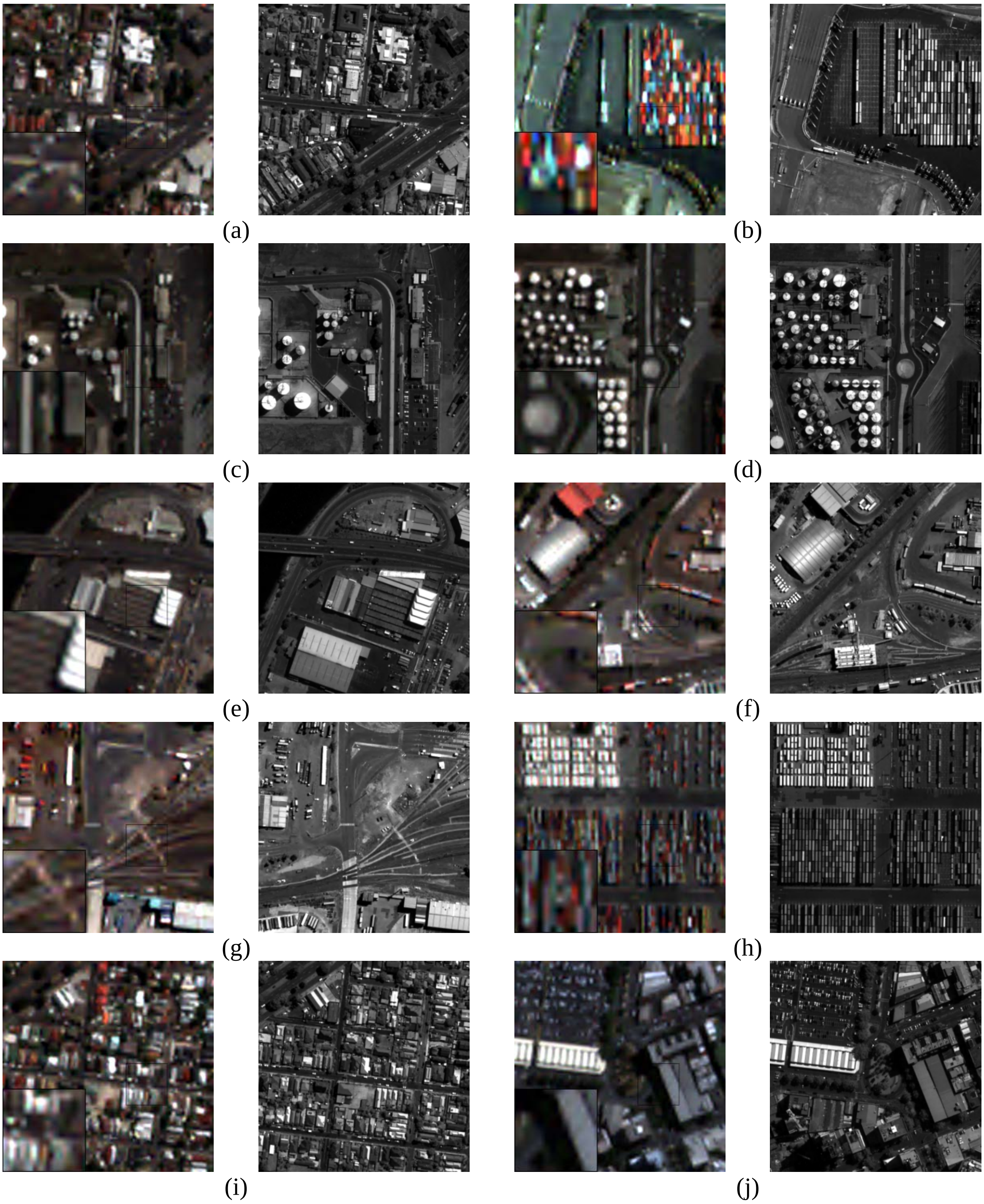

Figure 4. Ten pairs of panchromatic and multispectral Pleiades satellite dataset.

Table 2. Satellite images specification.

Band	Resolution (meter)	Projection	Datum	Date

Panchromatic	0.5	UTM, Lat. / Long.	WGS 84	04-05-2012
Four multispectral bands (Red, Green, Blue & NIR)	2			

4.2. Metrics

The visual analysis of the image does not represent the real quality analysis metric of images as it depends on human eyes, which are sensing different from an interpreter to another. In this paper the analysis is extended by using spatial and spectral metrics as illustrated in the following sections [3].

4.2.1. Quality with no reference (QNR) index. It calculates the distortion of image quality as a relation between the complement of spatial and spectral distortion multiplication D_λ and D_s respectively. Its value from zero to one, the higher value is the better.

4.2.2. Peak Signal to Noise Ratio (PSNR). It is the ratio between the intensity levels in the referenced source image and the related pixels in the fused image. The higher value of PSNR means higher quality.

$$PSNR = 10\log_{10}\frac{l^2}{\left(\frac{\sum_{i=1}^{m}\sum_{j=1}^{n}[FI(i,j)-R(i,j)]^2}{m\times n}\right)} \tag{12}$$

4.2.3. Standard Deviation (SD). It is a statistical measure that computes the diversity of the image as a contrast value that indicates the information availability in the image. The higher value is the better.

$$SD = \sqrt{\frac{\sum_{i=1}^{m}\sum_{j=1}^{n}(FI(i,j)-\mu_{FI})^2}{m\times n}} \tag{13}$$

4.2.4. Correlation Coefficient (CC). It measures statistically the strength and direction of the linear relationship between the referenced source image and the fused image. It indicates the spectral integrity if the reference image that is used is the multispectral image while it indicates the spatial integrity if the reference image that is used is high spatial image and then CC called spectral correlation coefficient (SCC). The ideal value is (+1) in range from [-1: 1].

$$\text{CC}= \frac{\sum_{i=1}^{m}\sum_{j=1}^{n}(FI(i,j)-\mu_{FI})(R(i,j)-\mu_R)}{\sqrt{\sum_{i=1}^{m}\sum_{j=1}^{n}((FI(i,j)-\mu_{FI})^2((R(i,j)-\mu_R))^2)}} \tag{14}$$

4.2.5. Entropy and Cross Entropy (ENT). They are statistical measures that indicate the information availability in the image. The higher value is the better.

$$ENT = -\sum_{g=1}^{L-1} p(g)\log_2 p(g) \tag{15}$$

4.2.6. Spatial Frequency (SF). It computes the spatial information level in both row and column directions. The higher value is the better.

$$RF = \sqrt{\frac{1}{m\times n}\sum_{i=1}^{m}\sum_{j=2}^{n}(FI(i,j)-R(i,j-1))^2} \tag{16}$$

$$CF = \sqrt{\frac{1}{m \times n} \sum_{i=2}^{m} \sum_{j=1}^{n} (FI(i,j) - R(i-1,j))^2} \tag{17}$$

$$SF = \sqrt{RF^2 + CF^2} \tag{18}$$

4.2.7. The blur effect. This metric is sensitive to focal and motion blur and also to edges, also it is sensitive to the presence of noise [20].

5. Results and evaluations

5.1. Subjective evaluation

As shown in figure 5, the fused images are obtained by seven different state-of-the-art fusion techniques either CS-based method (Brovey, Ehler, GS, HIS and PCA) or MRA-based method (DWT and CVT) are different in their spatial and spectral resolution according to the used fusion methods. In CS-based method generally, the main problem is the spectral deformation, while in MRA is the loss of spatial details. The proposed GS-CVT fusion method enhances the spectral information as well as enriches the spatial details. It is noticed that the fused images using the proposed technique have the best result visually in comparison with the other competing techniques.

(a)

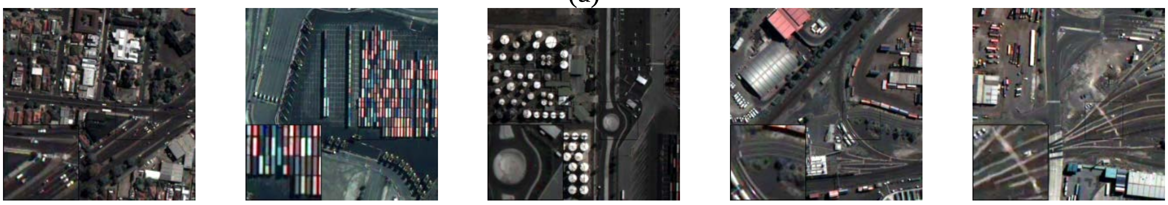

(b)

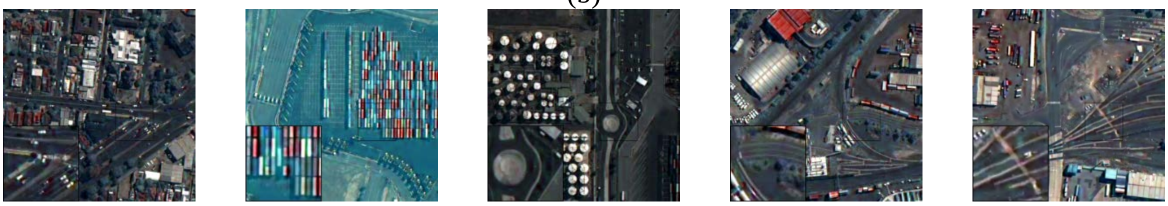

(c)

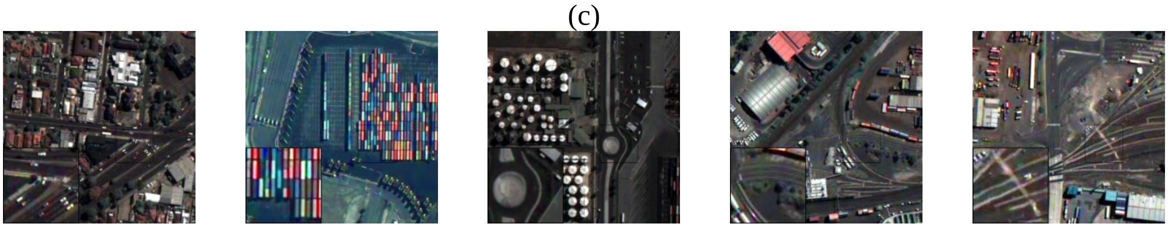

(d)

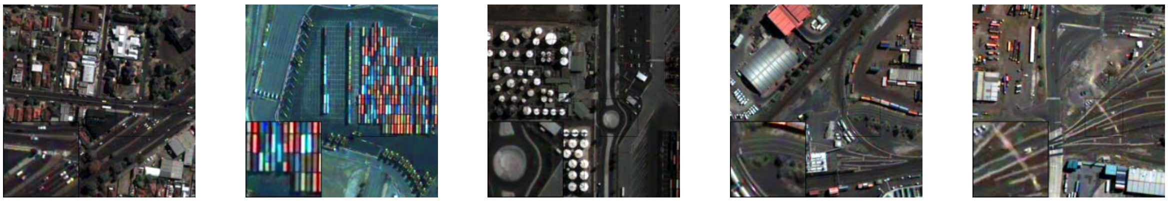

(e)

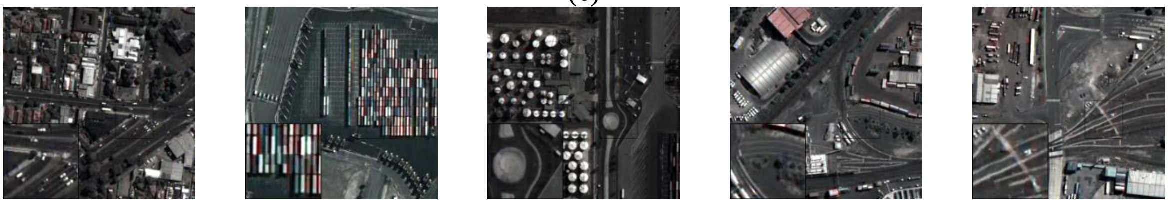

(f)

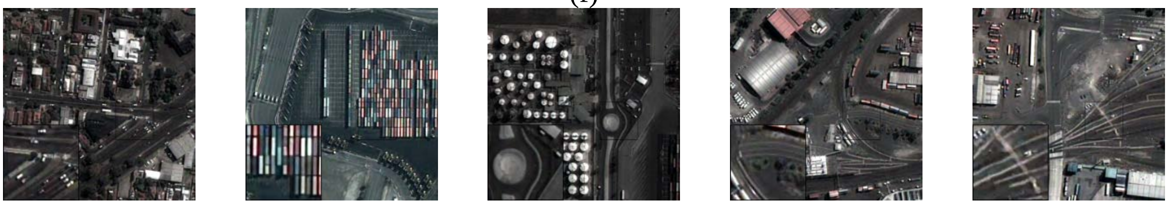

(g)

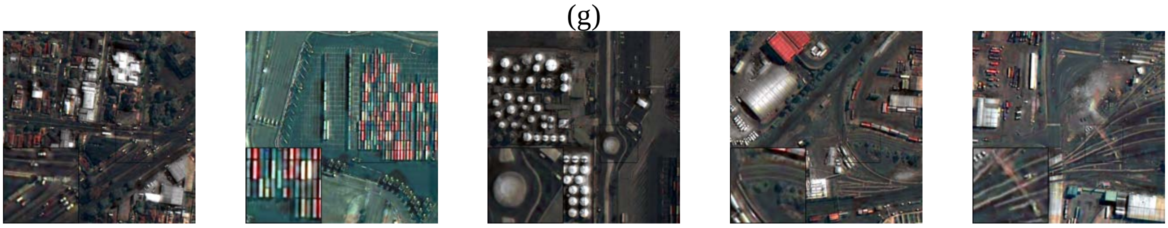

(h)

Figure 5. Example of applying different fusion techniques on Pleiades satellite dataset; (a) Brovey, (b) Ehler, (c) GS, (d) IHS, (e) PCA, (f) DWT, (g) CVT, (h) GS-CVT.

5.2. Objective evaluation

Table 3 shows the average values of objective evaluation metrics over the Pleiades benchmark-dataset, the proposed fusion method has the highest value of QNR that indicates minimum distortion; DWT and CVT have lower values and higher distortion. The proposed method has the highest value of PSNR indicates the high quality of the fused image followed by GS- based method then Brovey, the lowest value is DWT-based method as shown. CS-based methods have the lowest values of SD while the proposed method has the highest value that indicates its high contrast and image sharpener. For CC-metrics the best value is Ehler-based method followed by MRA-based method, then CS-based methods but for SCC the best value for the proposed method followed by MRA-based method, the CS-based methods. The measure of information availability ENT indicates that the proposed method has the highest value followed by MRA-based methods, the CS-based methods. Ehler-based method has the highest SF value followed by the proposed method, and the lowest values for the CS-based methods. The best blur values are assigned to MRA-based method followed by the proposed method, then CS-based method.

Table 3. Objective evaluation of fusion results.

Fusion method	blur	CC	SCC	Dλ	DS	QNR	Entropy	SF	PSNR	SD
PCA	0.343	0.976	0.777	0.063	0.237	0.716	1.646	6.248	40.166	228
IHS	0.344	0.978	0.767	0.073	0.242	0.704	0.649	6.103	40.43	228
Brovey	0.344	0.974	0.762	**0.053**	0.237	0.723	1. 659	5.913	40.584	229
Ehler	0.337	**0.99**	0.761	0.119	0.311	0.61	1.022	**11**	34.979	312
GS	0.334	0.944	0.731	0.086	0.242	0.694	1.73	6.943	40.716	246
DWT	0.320	0.985	0.769	0.16	0.313	0.581	1.917	8.695	34.894	305
CVT	**0.314**	0.983	0.788	0.164	0.295	0.594	1.858	9.855	35.981	289
GS-CVT	0.327	0.936	**0.804**	0.069	**0.219**	**0.728**	**2**	10	**41.992**	**329**

5.3. Competitive approaches

In this paper, the proposed GS-CVT-based method not only compared by the state-of-the-art methods but also compared with a newly published method that combines PCA and CVT methods [12]. The proposed method uses GS transform which is more generic than PCA in the hybrid fusion to overcome the radiometric accuracy shortage. Also the benefits from local fusion strategy that are proposed to make the fused image more robust than global fusion strategies. The comparison is done subjectively and objectively. The subjective evaluation indicates that PCA-CVT-based method is blurrier than this paper proposed method and also the spectral information are more preserved by the proposed method so the fused image looked more interpretable as shown in figure 6. It is worth mentioning that PCA-CVT method in [12] is implement by MATLAB where there is no open source code for it, also the used dataset for [12] is not uploaded, so there is no unified dataset.

(a) (b)

Figure 6. PCA-CVT-based method and GS-CVT-based method over sample Pleiades dataset.

It is clear from figure 6 that the GS-CVT-based method has sharpener image and good coloured compared to the other method. Table 4, represents different average values of objective evaluation metrics that reflect that PCA-CVT-based method can be objectively better than GS-CVT-based method in some metrics such as QNR, SCC, and Entropy while GS-CVT-based method is better in $CC, SD, SF, and\ Blur\ metrics$. From ranking table 3 and table 4 using the values of individual methods and their integration arranged such that best values take small values and the worst values take the large values in order as shown in figure 7, the proposed GS-CVT integration is the best that can improve the performance of the fusion process as it has the lowest value.

Table 4. Objective evaluation of fusion results by PCA-CVT and the proposed method.

Fusion method	blur	CC	SCC	QNR	Entropy	SF	PSNR	SD
GS-CVT	**0.327**	**0.936**	0.804	0.728	2	**10**	41.992	**329**
PCA-CVT	0.441	0.876	**0.962**	**0.864**	**2.068**	7	**43.937**	323

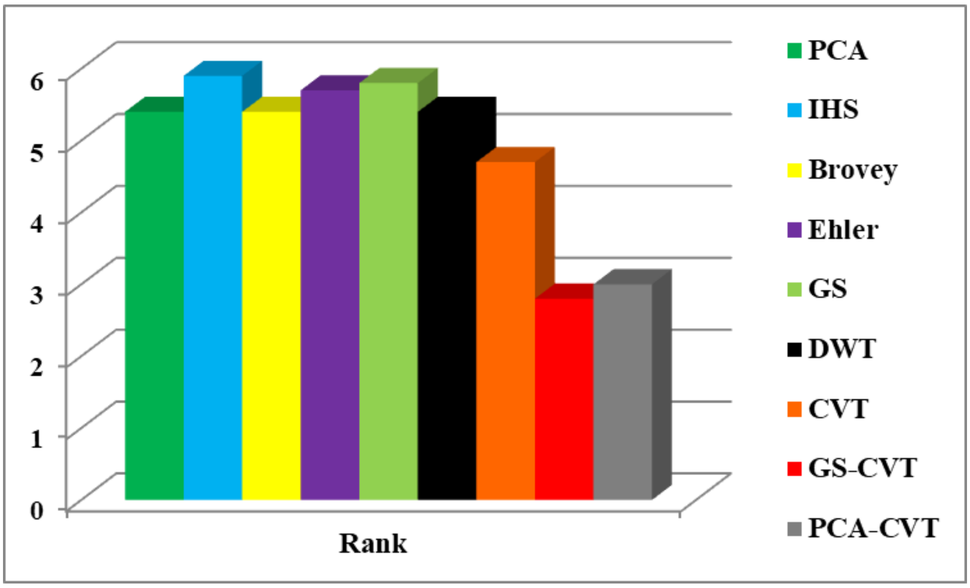

Figure 7. Ranking fusion methods in order

6. Conclusion

In this work, a proposed method based on GS and CVT methods is used in merging high spatial resolution panchromatic image and low spectral resolution multispectral image from remote sensing satellite Pleiades dataset. The fusion is done using a novel fusion rule that depends on predefined matching criteria over local window. The proposed method is compared with not only state-of-the-art methods but also a newly published work that combines PCA and CVT. The superiority of the proposed method is validated subjectively and objectively using $QNR, PSNR, CC, SCC, SD, SF, and\ Blur\ metrics$. The proposed method presents an efficient solution for fusion process of Pleiades satellite dataset, and provides high quality fused images spatially and spectrally.

7. Future work

Fusion process is a sophisticated operation that has different parameters as it can be done in many domains (spatial, frequency), and can be used in many applications using numerous types of images, etc. so traditional fusion methods are not the optimum fusion methods. It leads to using new fusion methods to get the optimum quality fused image. In order to estimate the optimum fused image we will take in consideration in future work to use the cost function in order to optimize the weights by using iterative methods based on statistical parameters to be more generalized in the fusion process.

Reference

[1] Pohl C and Van Genderen J 2016 *Remote sensing image fusion: a practical guide*: CRC Press

[2] Poobalasubramanian M, V S, Karthick S, Haribaabu V, Santhanam R and Samuel J 2020 A Review of Multi-resolution Analysis (MRA) and Multi-geometric Analysis (MGA) Tools Used in the Fusion of Remote Sensing Images *Circuits, Systems, and Signal Processing* **39**

[3] Kulkarni S and Rege P 2020 Pixel Level Fusion Techniques for SAR and Optical Images: A Review *Information Fusion* **59**
[4] Belgiu M and Stein A 2019 Spatiotemporal image fusion in remote sensing *Remote Sensing* **11** 818
[5] Ghamisi P, Rasti B, Yokoya N, Wang Q, Hofle B, Bruzzone L, Bovolo F, Chi M, Anders K and Gloaguen R 2018 Multisource and Multitemporal Data Fusion in Remote Sensing *arXiv preprint arXiv:1812.08287*
[6] Bhataria K C and Shah B K 2018 A Review of Image Fusion Techniques. In: *2018 Second International Conference on Computing Methodologies and Communication (ICCMC),* pp 114-23
[7] Imani M 2020 A collaborative representation-based approximation method for remote sensing image fusion *International Journal of Remote Sensing* **41** 974-95
[8] Liu K and Li Y 2019 SAR and multispectral image fusion algorithm based on sparse representation and NSST. In: *AIP Conference Proceedings*: AIP Publishing LLC p 020059
[9] Ma X, Hu S, Liu S, Fang J and Xu S 2019 Remote sensing image fusion based on sparse representation and guided filtering *Electronics* **8** 303-20
[10] Zhang W and Xu M 2019 Translate SAR data into optical image using IHS and wavelet transform integrated fusion *Journal of the Indian Society of Remote Sensing* **47** 125-37
[11] Dong L, Yang Q, Wu H, Xiao H and Xu M 2015 High quality multi-spectral and panchromatic image fusion technologies based on Curvelet transform *Neurocomputing* **159**
[12] Chen C, He X, Guo B, Zhao X and Chu Y 2020 A pixel-level fusion method for multi-source optical remote sensing image combining the principal component analysis and curvelet transform *Earth Science Informatics* 1-9
[13] Devulapalli S and Krishnan R 2019 Synthesized pansharpening using curvelet transform and adaptive neuro-fuzzy inference system *Journal of Applied Remote Sensing* **13** 034519
[14] Laben C A and Brower B V 2000 Process for enhancing the spatial resolution of multispectral imagery using pan-sharpening. Google Patents)
[15] Zhang D-D, Xie F and Zhang L 2018 Preprocessing and fusion analysis of GF-2 satellite Remote-sensed spatial data. In: *2018 International Conference on Information Systems and Computer Aided Education (ICISCAE)*: IEEE pp 24-9
[16] Yilmaz V, Serifoglu Yilmaz C, Güngör O and Shan J 2020 A genetic algorithm solution to the gram-schmidt image fusion *International Journal of Remote Sensing* **41** 1458-85
[17] Chen C, He X, Chu Y and Zhao X 2020 A new remote sensing image fusion method combining principal component analysis and curvelet transform *MS&E* **780** 032054
[18] Candès E, Demanet L, Donoho D and Ying L 2006 Fast Discrete Curvelet Transforms *SIAM Journal on Multiscale Modeling and Simulation* **5**
[19] Harrisgeospatial.com. 2021. L3Harris Geospatial | Remote Sensing Technologies | Geospatial Data and Imagery.
[20] Crété-Roffet F, Dolmière T, Ladret P and Nicolas M 2007 The Blur Effect: Perception and Estimation with a New No-Reference Perceptual Blur Metric *Human Vision and Electronic Imaging* **12**